

# Empirical regularities in the $x$ -dependence of nuclear $J/\Psi$ suppression

C.Gerschel<sup>1</sup>, J. Hüfner<sup>2</sup> and E.Quack<sup>3</sup>

<sup>1</sup> Institut de Physique Nucléaire, 91406 Orsay Cedex, France

<sup>2</sup>Institut für Theoretische Physik der Universität,  
Philosophenweg 19, 69120 Heidelberg, Germany

<sup>3</sup> Theoret. Physik, Gesellschaft für Schwerionenforschung (GSI),  
P.O.Box 11 05 52, 64220 Darmstadt, Germany

January 1995

## Abstract

The measured ratios  $R(x, A_1/A_2)$  for  $J/\Psi$ ,  $\Psi'$  and  $\mu^+\mu^-$  production on two different targets  $A_1, A_2$  as a function of the fractional momentum  $x$  of the final state are well fit with a very simple functional form having three adjustable parameters. An empirical relation is found between the three parameters of the fit. The deduced  $J/\Psi$  absorption cross sections  $\sigma_{abs}$  cluster around two values of which only  $\sigma_{abs} = 5.8 \pm 0.2$  mb seems acceptable.

With the advent of complete  $\mathcal{O}(\alpha_s^3)$  calculations [1, 2], the production of charm states in hadronic collisions like  $hp \rightarrow J/\Psi X$  is approaching a quantitative understanding. When produced in a nucleus, however, deviations from the extrapolation of  $hp$  reactions are observed [3] – [6] which are likely to be of a nonperturbative origin. Many explanations have been proposed of which we quote only a few [7] – [10]. No definite conclusion on the mechanism can be drawn at the present time. The understanding of  $hA$  collisions is of great importance as it provides a reference for  $J/\Psi$  production in nucleus–nucleus collisions, in connection with the search for quark–gluon–plasma formation.

While in the direction transverse to the beam an observed broadening of the  $p_\perp$  distribution seems to be understood in terms of multiple scattering of the initial partons [11], the nature of the observed longitudinal momentum dependence remains mysterious. In the present work, we concentrate on the latter one and present an analysis of the experimental data which is completely unbiased by theoretical models. In this purely empirical way we find surprising regularities which seem general to all the existing data.

Data are published using the kinematic variable  $x_F = p_\parallel/p_\parallel^{max}$  in the hadron–nucleon center–of–mass system (cms), and in this work we consider  $p_\perp$ -integrated data only. Mass  $M$  and  $x_F$

of the produced state can be related to the Bjorken variables  $x_1$  and  $x_2$  of the partons in the projectile and target hadrons, respectively, by  $x_F = x_1 - x_2$  and  $M^2 = x_1 x_2 s$  when projectile and nucleon masses are neglected and where  $\sqrt{s}$  is the cms energy in the  $hN$  system. Inverting these relations,

$$x_{1,2} = \frac{1}{2}[\pm x_F + \sqrt{x_F^2 + 4M^2/s}] \quad (1)$$

allows us to convert the observed values of  $M^2$  and  $x_F$  into the variables  $x_1$  and  $x_2$ .  $M$  refers to the mass of the produced state  $H$  ( $H = J/\Psi$ ,  $\Psi'$  or  $\mu^+\mu^-$ ).

In the following, we study the ratio  $R$  of the production cross sections on two different target nuclei  $A_1$  and  $A_2$ , where  $x$  stands for one of the variables  $x_1$ ,  $x_2$  or  $x_F$ ,

$$R_{hH}(x, A_1/A_2) = \frac{\frac{1}{A_1} \frac{d\sigma}{dx}(hA_1 \rightarrow HX)}{\frac{1}{A_2} \frac{d\sigma}{dx}(hA_2 \rightarrow HX)} \equiv A_1^{\alpha(x,A_1)-1} / A_2^{\alpha(x,A_2)-1} . \quad (2)$$

We use the notation  $R_{hH}(x, A)$  when dealing with a comparison of  $hA$  with  $hp$  data ( $A_1 = A, A_2 = 1$ ). In the frequently used parametrization  $A^\alpha$ ,  $\alpha$  is the effectiveness of the nucleus  $A$  to produce the heavy final state  $H$  from the projectile  $h$ ; a value of  $\alpha$  (or  $R$ )  $< 1$  indicates a suppression.

While  $\alpha = 1$  is expected from a perturbative calculation of heavy final state production, experimentally a suppression is observed which increases with  $x_F$ . The data show relative small effects ( $1 - \alpha \leq 0.02$ ) for Drell–Yan dimuon pairs ( $m_{\mu\mu} \geq 4$  GeV) [12]. The suppression is more sizable for  $J/\Psi$  and  $\Psi'$  production. Here,  $1 - \alpha \approx 0.05 - 0.09$  for small values of  $x_F$  and increases to  $1 - \alpha \approx 0.2$  at large  $x_F$  [3] – [6].

When experimental cross sections are concerned, the ratio eq.(2) is denoted by  $R_{hH}^{\text{ex}}(x, A_1/A_2)$ . Here, the incoming hadron  $h$  may be a proton, pion or antiproton, and the final state  $H$  a  $J/\Psi$ ,  $\Psi'$  or a  $\mu\mu$  pair with given  $M^2$ . The experimental cross section ratios  $R^{\text{ex}}(x, A_1/A_2)$  form the basis of our analysis [3] – [6]. We disregard several older experiments with very low statistics or a small acceptance range in  $x_F$ . Altogether, the data come from 22 different reactions with a total statistics of about  $3 \cdot 10^6$  events. The statistics differs strongly from reaction to reaction, and correspondingly do the errors on the parameter values which we will obtain. We use the errors  $\Delta R_{hH}^{\text{ex}}(x, A_1/A_2)$  as they are given in the papers, although it is not always clear to which degree they include systematic uncertainties.

Several models have been proposed in order to explain the observed  $x_F$ –dependence, among them parton energy loss in the initial state [7], shadowing of the parton distribution entering the hard fusion process [8], final state absorption [9] and intrinsic charm in the projectile  $h$  [10]. The assembly of these effects was considered in works such as [13, 14]. In a previous study [15], we have analyzed the existing data in the light of these theoretical models with the aim to discriminate between the various proposed mechanisms. This attempt remained unsatisfactory since the theoretical results did not describe the data well, i.e. resulted in an intolerable high  $\chi^2$ , and the fits to different data sets were not always consistent. In this paper we present a purely empirical study, void of any theoretical prejudices, in which we try to find the best parametrization of the data.

We have analyzed experiments which differ in the projectile hadron, its energy, in the target nuclei and in the final state ( $J/\Psi$ ,  $\Psi'$  and  $\mu\mu$ ). The data for the ratio  $R(x, A)$  where  $x = x_1$  or  $x = x_F$  show two rather distinct regimes. For low  $x$ , the ratio  $R$  is approximately constant, while

it drops quite rapidly with  $x$  at high  $x$ . In order to investigate this property more quantitatively, we parametrize the ratio  $R(x, A)$  in the following form

$$R_{hH}^{\text{fit}}(x, A) = A^{\alpha-1} \cdot [1 - b(x - x_0)\Theta(x - x_0)] \quad (3)$$

with three adjustable parameters, the absorption coefficient  $\alpha$ , the slope  $b$  and the break point  $x_0$ . As usual,  $\Theta(x) = 0$  for  $x < 0$  and  $\Theta(x) = 1$  for  $x \geq 0$ . The functional form represented by Eq.(3) consists of two straight lines intersecting at  $x = x_0$ : A horizontal line for  $x < x_0$  and a falling straight line with slope  $b$  for  $x \geq x_0$ .

By varying the parameters in Eq.(3), we perform a least  $\chi^2$  fit to the corresponding data set, i.e. we minimize the expression for  $\chi^2$  per degree of freedom,

$$\chi_{\text{pdf}}^2(\alpha, b, x_0) = \frac{1}{N_{\text{pts}} - N_{\text{par}}} \sum_{i=1}^{N_{\text{pts}}} \left[ \frac{R^{\text{fit}}(x^i, A_1/A_2; \alpha, b, x_0) - R^{\text{ex}}(x^i, A_1/A_2)}{\Delta R^{\text{ex}}(x^i, A_1/A_2)} \right]^2, \quad (4)$$

with respect to the parameters  $\alpha, b$  and  $x_0$ . Here,  $x$  may be  $x_1$  or  $x_F$ , the upper index  $i$  runs over the  $N_{\text{pts}}$  data points measured in a particular reaction, and  $N_{\text{par}} = 3$ . The minimization is done numerically using the routine MINUIT [16]. The errors to the parameters are also calculated with this routine and represent the variance in each of the parameter values for a change of  $\chi^2$  from the minimum value  $\chi_{\text{pdf}}^2$  to  $\chi_{\text{pdf}}^2 + 1$ .

The results of this procedure are shown in Table 1 for the data [3] – [6] and for  $x = x_1$ . The results for  $x = x_F$  are not significantly different from these. An ideal fit would give a value  $\chi_{\text{pdf}}^2 = 1$ . The values for  $\chi_{\text{pdf}}^2$  in Table 1 are mostly smaller than 1, which is probably due to the inclusion of systematic errors into the quoted errors of the data. The rather small values of  $\chi_{\text{pdf}}^2$  indicate that the parametrization by Eq.(3) is sufficiently flexible to adjust well to the data. Two representative fits are shown in Fig. 1.

Table 1 contains the values for the parameters  $\alpha, b$  and  $x_0$ , which appear in the fit formula Eq.(3). The table also displays two other parameters, the absorption cross section  $\sigma_{\text{abs}}$  and the intercept  $y_0$ , which are functions of the fit parameters.

The absorption cross section is an effective parameter which can be deduced from  $\alpha$  through the relation

$$A^{\alpha-1} = e^{-L\sigma_{\text{abs}}\rho_0} \quad (5)$$

where  $\rho_0$  is the density of nuclear matter and  $L$  the mean length of the trajectory of the produced particle in the final state.  $\sigma_{\text{abs}}$  is an effective cross section as it describes the interaction with nuclear matter of either the embryonic  $c\bar{c}$  [14] or of the final  $J/\Psi$  or  $\Psi'$ . Approximate formulae for  $L$  are given by [9],

$$L = \begin{cases} \frac{A-1}{A} \frac{3}{4} r_0 A^{\frac{1}{3}} & A \geq 40 \\ \frac{A-1}{\rho_0} \frac{3}{8\pi} \frac{1}{\langle r^2 \rangle} & A < 40 \end{cases}. \quad (6)$$

Here,  $\langle r^2 \rangle$  stands for the experimental mean square charged radius. We use  $r_0 = 1.2$  fm and  $\rho_0^{-1} = 4\pi r_0^3/3$ .

The intercept  $y_0$  is defined as follows. One considers only the falling straight line in Eq.(3) and denotes it by

$$y(x) = A^{\alpha-1} \cdot (1 - b(x - x_0)). \quad (7)$$

Then, extrapolating  $y(x)$  to the point  $x = 0$  (where  $y(x)$  should not describe the data), one has

$$y_0 \equiv y(0) = A^{\alpha-1} \cdot (1 + bx_0), \quad (8)$$

which depends on the parameters  $\alpha$ ,  $b$  and  $x_0$ . In Fig. 1, the extrapolation  $y(x)$  is shown by the dashed line.

We discuss the results shown in Table 1 and concentrate mainly on the  $J/\Psi$  data:

- (i) The values of the parameters do not display any systematic correlation with the energy of the projectile. This phenomenon is called scaling. The data are not sufficiently precise to distinguish between scaling in  $x_1$  or  $x_F$ . The reason for this difficulty is the following. The suppression is constant, i.e. independent of  $x$  for small  $x_1$  or  $x_F$ , where these variables differ. A significant  $x$ -dependence is observed only above  $x_0 \approx 0.3$ , where  $x_1 \approx x_F$ . Therefore,  $R(x, A)$  is within the error bars not sensitive to the choice  $x_1$  or  $x_F$ . However, the observed scaling in  $x_1$  or  $x_F$  implies strong scaling violations in  $x_2$ , as has been pointed out already in [17] on the basis of fewer data.
- (ii) One cannot recognize any systematic variations in the parameter values which correlate with the different projectiles  $p, \pi$  and  $\bar{p}$ . However, there are strong effects depending on whether the reference cross section in the denominator of Eq.(2) is measured on a proton ( $A_2 = 1$ ) or on a larger nucleus ( $A_2 \geq 2$ ).
- (iii) The data seem to indicate

$$y_0 = 1. \quad (9)$$

within the error bars. Of the 14 different experimental values 9 fulfill the relation Eq.(9) within one standard deviation, while only two are significantly outside the 2 standard deviation limit. Therefore we are rather confident about the validity of the Eq.(9), which relates the three fit parameters  $\alpha, b$  and  $x_0$  to each other. The physical significance of the empirical result, Eq.(9), is unclear to us. At present it indicates that the nuclear effects in the  $J/\Psi$  production from nuclei can basically be described by *two* parameters only.

- (iv) The empirical values for the absorption parameter  $1 - \alpha$  or equivalently the absorption cross section  $\sigma_{abs}$  show large fluctuations. A closer inspection reveals the following systematics: The absorption cross sections deduced from the experiments where nuclear data  $hA$  are related to  $hp$  ones with protons as targets cluster around a value of

$$\overline{\sigma}_{abs}^{(1)} = 3.2 \pm 0.5 \text{mb} \quad (10)$$

where 4 out of the 5 experimental values are compatible with  $\overline{\sigma}_{abs}^{(1)}$  within one standard deviation. The other data, where the  $hA_1$  results are related to  $hA_2$  with  $A_2 = 2$  or 9 cluster around

$$\overline{\sigma}_{abs}^{(2)} = 5.8 \pm 0.2 \text{mb} \quad (11)$$

where 6 out of the 9 data points are compatible with  $\overline{\sigma}_{abs}^{(2)}$  within one standard deviation.

The values  $\bar{\sigma}_{abs}^{(1)}$  and  $\bar{\sigma}_{abs}^{(2)}$  are incompatible with each other within their error bars, thus the classification into two groups may indicate a physical effect: The two data sets deduced from  $R(x, A/1)$  and  $R(x, A_1/A_2)$ ,  $A_2 > 1$  differ in their reference, one being the production on a proton, the other on a small nucleus having equal or nearly equal number of protons and neutrons. The data with  $A_2 = 1$  all come from the NA3 experiment [3], while the other experiments give only ratios with  $A_2 \geq 2$ . In order to clarify the origin of the discrepancy in the two values for  $\sigma_{abs}$ , we also use data for *absolute*  $x_F$ -integrated  $J/\Psi$  production cross sections on various targets.

The absolute cross sections of  $J/\Psi$  production per nucleon measured for  $pp$ ,  $pA$  and  $A_1A_2$  reactions at different projectile energies are extrapolated to 200 GeV/nucleon by using the well established empirical Craigie formula [18]

$$\sigma/\text{nucleon} \propto \exp\left(\frac{-14.5M}{\sqrt{s}}\right).$$

These cross sections are given for  $x_F > 0$  and  $\cos\theta_{CS}$  ranging from -1 to 1 where  $\cos\theta_{CS}$  is the Collins–Soper angle of the muon pair. When they are plotted against the length  $L$  of the trajectory in the final state, they fall on one exponential curve with the exception of the  $pp$  reaction (NA3). This is shown in Fig. 2. Extrapolating the dashed line in Fig. 2 to  $L = 0$  (no absorption), one deduces a value of  $\sigma = 4.4$  nb for  $J/\Psi$  production in a  $pN$  reaction, where  $N$  stands for the average of  $pp$  and  $pn$ . This is off by two standard deviations from the  $pp$  result. Though unexpected, this result is not in contradiction with fundamental symmetries, since  $pp$  has isospin  $I = 1$  only, while  $I = 0$  and  $I = 1$  contribute to  $pn$  reactions. Yet the dominance of gluon fusion in  $J/\Psi$  production makes such large differences in  $I = 1$  and  $I = 0$  appear very unlikely. Therefore we have to conclude that the proton target data have a specific behavior in the NA3 experiment.

With the exception of the  $pp$  point at  $L = 0$ , all data shown in fig. 2 fall on an exponential line whose slope is related to an absorption cross section of  $\sigma_{abs} = 5.9 \pm 1.4$  mb via Eq.(5). This value is very close to the value  $\sigma_{abs}^{(2)}$  extracted from the data shown in table 1. Only part of the experimental data are in common between table 1 and fig. 2, as differential cross sections  $d\sigma/dx_F$  are not available for all systems.

Our discussion has shown that the  $hp$  data fall out of the systematics for  $hA$  data when extrapolated to  $A \rightarrow 1$ . Therefore we discard the value for  $\bar{\sigma}_{abs}^{(1)}$  as an absorption cross section. Then the analysis based on Table 1 and Fig. 2 yield a value

$$\bar{\sigma}_{abs}^{J/\Psi N} = 5.8 \pm 0.2 \text{mb}. \quad (12)$$

As can be seen in Table 1, most of the deviations from the empirical law occur for the data from NA3, which seem to have a problem with the normalization. When correcting for the overall normalization of the NA3 data by using the value of  $\bar{\sigma}_{abs}^{J/\Psi N}$ , Eq.(12), the results for  $y_0$  are correspondingly shifted downwards and become compatible with the observed systematics of  $y_0 = 1$  from the other data sets.

Finally, we plot in Fig. 3 the ratios  $R(x, A_1/A_2)/(A_1/A_2)^{\alpha-1}$ , where  $\alpha$  is given in table 1. The normalization via the factor  $(A_1/A_2)^{\alpha-1}$  corrects for any possible discrepancies in the absolute normalization of the  $hp$  data. Only data are compared where  $A_1$  is heavy (184 or 195) and  $A_2$  is light (1,2 or 9). The solid line on the figure is a fit to the  $x_1$  dependence of the data using Eq.(3). The similarity of the behavior of the different systems is striking despite different projectiles and projectile energies and thus shows the degree of scaling.

The data for  $\Psi'$  production, measured only at 800 GeV, yield also an absorption cross section of  $\bar{\sigma}_{abs}^{\Psi'} = 5.8 \pm 0.6$  mb which is the same as for the  $J/\Psi$  final state. Since  $J/\Psi$  and  $\Psi'$  differ in their size and since the absorption cross section should depend on the radius, the equality of the absorption cross sections is not obvious. The explanation provided in ref.[14] is seducing but does not account for all the regularities presented in this paper. The systematics  $y_0 = 1$  is always fulfilled for the  $\Psi'$  within the error bars.

The data for  $\mu^+\mu^-$  production yield absorption cross sections compatible with zero – as it should be. The systematics of  $y_0$  is unclear.

We summarize for the  $J/\Psi$  production on nuclei:

1. The data for the  $x_1$  (or  $x_F$ )–distribution of  $J/\Psi$  production on nuclei,  $R(x, A_1/A_2)$ , can well be fit by a simple functional dependence of two intersecting straight lines

$$R^{\text{fit}}(x, A) = A^{\alpha-1} \cdot [1 - b(x - x_0)\Theta(x - x_0)] \quad (13)$$

with three parameters  $\alpha, b$  and  $x_0$ .

2. The parameters do not display any visible correlation with the type of projectile nor its energy and thus show  $x_1$  or  $x_F$  scaling.
3. The falling straight line of the parametrization when extrapolated to  $x = 0$  takes the value  $y_0 = 1$  or

$$1 = A^{\alpha-1} \cdot (1 + b x_0) \quad (14)$$

This empirical result seems well established, but its physical meaning is not understood.

4. The absorption cross sections  $\sigma_{abs}$  deduced from the fitted values for  $\alpha$  cluster around two distinctly different values  $\bar{\sigma}_{abs}^{(1)}$  and  $\bar{\sigma}_{abs}^{(2)}$  depending on whether they are deduced from data for  $R(x, A/1)$  or  $R(x, A_1/A_2)$ ,  $A_2 > 1$ , respectively. We argue that only  $\bar{\sigma}_{abs}^{(2)} = 5.8 \pm 0.2$  mb can be interpreted as an absorption cross section for  $J/\Psi$  propagation in nuclear matter.
5. The data for  $J/\Psi$  suppression in *nucleus–nucleus* collisions, also displayed in Fig. 2, follow the same systematics as the  $pA$  data, in that a common absorption cross section of  $\sigma_{abs}^{J/\Psi N} = 5.9 \pm 1.4$  mb describes all data. This implies that so far no extra effects are seen in nucleus–nucleus collisions which are not yet present in proton–nucleus ones.

### Acknowledgments

We thank J.Dolejsi for his help with the minimization procedure. This work has been supported in part by the BMFT under contract no. 06 HD 742.

## References

- [1] P. Nason, S. Dawson and R.K. Ellis, Nucl. Phys. B303 (1988) 607; B327 (1989) 49; M.L. Mangano, P. Nason and G. Ridolfi, Nucl. Phys. B373 (1992) 295
- [2] W. Beenakker, H. Kuijf, W.L. van Neerven, and J. Smith, Phys. Rev. D40 (1989) 54; W. Beenakker, W.L. van Neerven, R. Meng, G.A. Schuler, and J. Smith, Nucl. Phys. B351 (1991) 507
- [3] NA3–Collab., J.Badier et al., Z. Phys. C 20 (1983) 101
- [4] E772–Collab., D.M.Alde et al., Phys. Rev. Lett. 66 (1991) 133
- [5] E537–Collab., C.Akerlof et al., Phys. Rev. D 48 (1993) 5067
- [6] E789–Collab., M.Kowitt et al., Phys. Rev. Lett. 72 (1994) 1318
- [7] B.Kopeliovich and F.Niedermayer, Dubna preprint JINR-E2-84-834 (1984)
- [8] S.Gupta and H.Satz, Z.Phys. C 55 (1992) 391
- [9] C.Gerschel and J.Hüfner, Z. Phys. C 56 (1992) 171
- [10] S.J.Brodsky and P.Hoyer, Phys. Rev. Lett. 63 (1989) 1566
- [11] J. Hüfner, Y. Kurihara and H.J. Pirner, Phys. Lett. B 215, 218 (1988); S. Gavin and M. Gyulassy, Phys Lett. B 214, 241 (1988); J.-P. Blaizot and J.-Y. Ollitrault, Phys. Lett. B 217 (1989) 392
- [12] E772–Collab., D.M.Alde et al., Phys. Rev. Lett. 64 (1990) 2479
- [13] R. Vogt, S. Brodsky and P. Hoyer, Nucl. Phys. B 360 (1991) 67
- [14] D.Kharzeev and H.Satz, Z.Phys. C 60 (1993) 389
- [15] C.Gerschel, J. Hüfner and E.Quack, ‘Phenomenological analysis of the  $x$ -distribution for  $J/\Psi$  production on nuclei’, preprint HD–TVP–94–1 (unpublished)
- [16] MINUIT, CERN program library long writeup D506, March 1992
- [17] P.Hoyer, M.Vänttinen and U.Sukhatme, Phys. Lett. B 246 (1990) 217
- [18] N.S.Craigie, Phys. Rep. 47 (1978) 1
- [19] L.Antoniazzi et al., E705 Collab., Phys. Rev. D 46 (1992) 4828
- [20] K.J.Anderson et al., Phys. Rev. Lett. 42 (1979) 944
- [21] C.Baglin et al., Phys. Lett. B 270 (1991) 105

## Figure Captions

### Fig. 1

Left: The ratios  $R(x, A)$  for  $\pi Pt \rightarrow J/\Psi$  relative to  $\pi p \rightarrow J/\Psi$  at 150 GeV from the NA3 experiment [3], Right:  $R(x, W/D)$  at 800 GeV from the experiment E772 [4]. Both data sets are plotted as a function of  $x_1$  and fitted by the parametrization eq.(3). The extrapolation of the falling straight line to the intercept  $y(0)$  is indicated by the dashed lines.

### Fig. 2

Plot of  $J/\Psi$  production cross sections/nucleon times branching ratio  $B(J/\Psi \rightarrow \mu\mu)$  for  $pA$  and  $A_1A_2$  collisions as a function of the mean length  $L$  (in fm) of matter in the final state. All data [3, 5], [19] – [21] are extrapolated to  $\sqrt{s} = 19.4$  GeV. The exponential fit (dashed line) provides an absorption cross section of 5.9 mb.

### Fig. 3

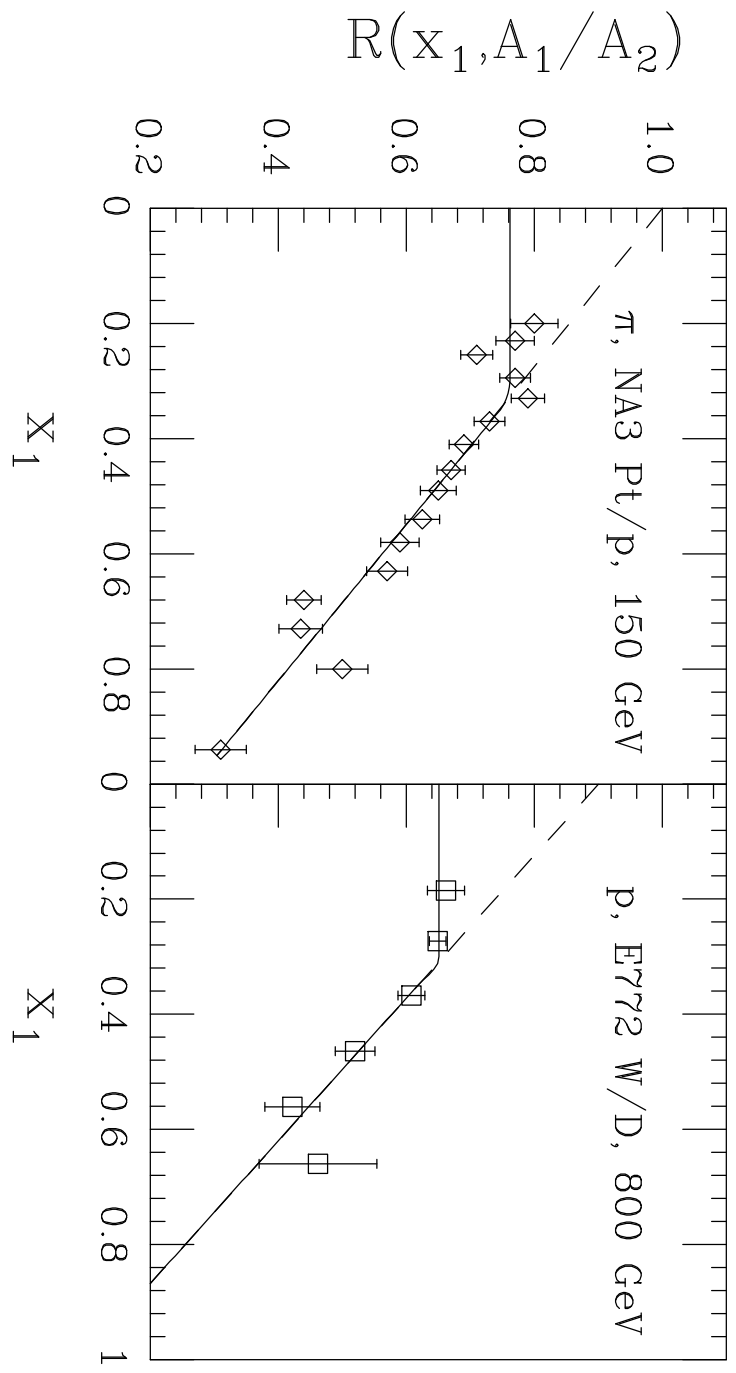
Ratios  $R(x, A_1/A_2)/(A_1/A_2)^{\alpha-1}$  plotted as a function of  $x_1$ . Data for  $A_1 = 184$  and 195 and  $A_2 = 1, 2, 9$  are fitted by the parametrization of Eq.(3).

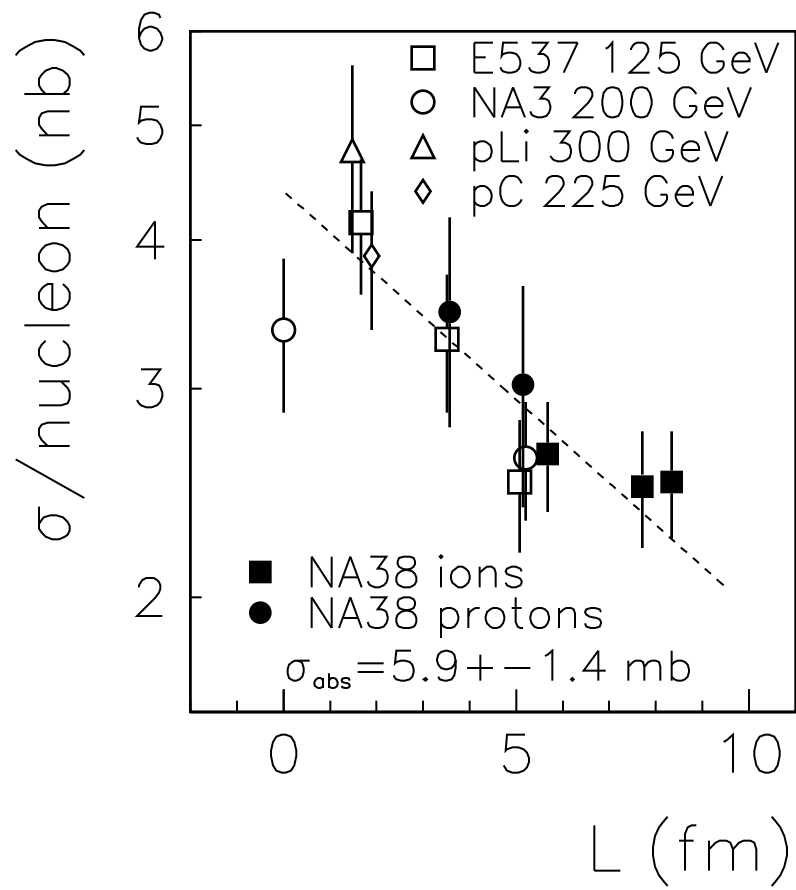


Reaction				Parameters of fit				Deduced quantities	
$H$	$h$	$E_{Lab}$	$A_1/A_2$	$\alpha$	$b$	$x_0$	$\chi_{pdf}^2$	$\sigma_{abs}$ [mb]	$y_0$
$J/\Psi$	$p$	200	195/1 <sup>a</sup>	$0.944 \pm 0.005$	$-2.4 \pm 0.6$	$0.42 \pm 0.03$	0.6	$4.15 \pm 0.40$	$1.51 \pm 0.20$
		800	12/2 <sup>b</sup>	$0.952 \pm 0.018$	$-0.5 \pm 0.2$	$0.25 \pm 0.09$	0.4	$5.02 \pm 1.84$	$1.00 \pm 0.06$
			40/2 <sup>b</sup>	$0.942 \pm 0.003$	$-4.1 \pm 10.5$	$0.57 \pm 0.51$	0.4	$5.50 \pm 0.27$	$2.67 \pm 5.12$
			56/2 <sup>b</sup>	$0.934 \pm 0.003$	$-1.3 \pm 0.7$	$0.39 \pm 0.07$	0.4	$5.95 \pm 0.26$	$1.16 \pm 0.23$
			184/2 <sup>b</sup>	$0.918 \pm 0.003$	$-1.2 \pm 0.3$	$0.31 \pm 0.04$	0.5	$6.30 \pm 0.27$	$0.90 \pm 0.07$
			64/9 <sup>c</sup>	$0.938 \pm 0.718$	$-0.4 \pm 0.6$	$0.32 \pm 0.65$	2.9	$3.38 \pm 39.46$	$1.00 \pm 0.29$
	$\bar{p}$	125	64/9 <sup>d</sup>	$0.923 \pm 0.013$	$0.7 \pm 0.5$	$0.36 \pm 0.00$	4.1	$4.26 \pm 0.73$	$0.65 \pm 0.14$
			184/9 <sup>d</sup>	$0.885 \pm 0.007$	$-2.7 \pm 1.9$	$0.59 \pm 0.06$	0.6	$6.08 \pm 0.35$	$1.85 \pm 0.79$
	$\pi^-$	125	64/9 <sup>d</sup>	$0.990 \pm 0.559$	$-0.3 \pm 0.9$	$0.22 \pm 0.53$	4.2	$0.57 \pm 30.70$	$1.05 \pm 0.26$
			184/9 <sup>d</sup>	$0.818 \pm 0.015$	$-1.1 \pm 0.2$	$0.42 \pm 0.03$	7.4	$8.99 \pm 0.73$	$1.21 \pm 0.08$
	$\pi^-$	150	195/1 <sup>a</sup>	$0.948 \pm 0.002$	$-1.0 \pm 0.0$	$0.33 \pm 0.00$	1.5	$3.80 \pm 0.17$	$1.00 \pm 0.01$
	$\pi^-$	200		$0.977 \pm 0.005$	$-1.4 \pm 0.4$	$0.40 \pm 0.05$	0.2	$1.69 \pm 0.39$	$1.39 \pm 0.16$
	$\pi^+$			$0.958 \pm 0.005$	$-0.7 \pm 0.4$	$0.34 \pm 0.10$	0.4	$3.07 \pm 0.37$	$1.00 \pm 0.13$
	$\pi^-$	280		$0.960 \pm 0.003$	$-1.1 \pm 0.1$	$0.32 \pm 0.02$	0.9	$2.91 \pm 0.21$	$1.09 \pm 0.03$
$\Psi'$	$p$	800	12/2 <sup>b</sup>	$0.947 \pm 0.018$	$-0.9 \pm 0.6$	$0.28 \pm 0.00$	5.0	$5.54 \pm 1.86$	$1.10 \pm 0.15$
			40/2 <sup>b</sup>	$0.950 \pm 0.011$	$-1.5 \pm 0.5$	$0.20 \pm 0.08$	1.0	$4.69 \pm 1.07$	$1.09 \pm 0.12$
			56/2 <sup>b</sup>	$0.930 \pm 0.011$	$-1.5 \pm 0.8$	$0.34 \pm 0.06$	0.8	$6.37 \pm 0.98$	$1.14 \pm 0.20$
			184/2 <sup>b</sup>	$0.917 \pm 0.010$	$-1.0 \pm 1.3$	$0.31 \pm 0.17$	0.3	$6.37 \pm 0.73$	$0.85 \pm 0.29$
$\mu\mu$	$p$	800	12/2 <sup>e</sup>	$1.002 \pm 0.003$	$-0.9 \pm 0.8$	$0.64 \pm 0.06$	0.9	$-0.24 \pm 0.31$	$1.55 \pm 0.55$
			40/2 <sup>e</sup>	$1.011 \pm 0.122$	$-0.2 \pm 0.1$	$0.15 \pm 0.54$	0.5	$-0.99 \pm 11.43$	$1.07 \pm 0.10$
			56/2 <sup>e</sup>	$1.000 \pm 0.002$	$-0.1 \pm 0.1$	$0.35 \pm 0.00$	1.8	$0.03 \pm 0.14$	$1.05 \pm 0.02$
			184/2 <sup>e</sup>	$0.998 \pm 0.001$	$-0.7 \pm 0.3$	$0.53 \pm 0.05$	0.3	$0.17 \pm 0.11$	$1.33 \pm 0.18$

Table 1:

Result of the  $\chi^2$  fit of the test function, Eq.(3), to the experimental ratios  $R_{hH}(x_1, A_1/A_2)$ , Eq.(1). Data are of ref. [3] for <sup>a</sup>), [4] for <sup>b</sup>), [5] for <sup>c</sup>), [6] for <sup>d</sup>) and [12] for <sup>e</sup>). Here,  $H$  stands for the final state produced in the reaction,  $h$  for the projectile, and  $A_1$  and  $A_2$  denote the two targets. The parameters of the fit are listed in the middle columns, together with the corresponding  $\chi_{pdf}^2$ , and the deduced quantities (see text) are shown in the two last columns.





Global fit to J/ $\psi$  data scaled to  $A^{\alpha-1}$  for  $A_1 > 180$

